Molecular Geometries and Electronic Structures of Methyl Pyropheophorbide-a and (Cationic) Tropolonyl Methyl Pyropheophorbides: DFT Calculation

Na-Ri Kim, Sujin Kim, Jin Dong Kim, Do Sung Huh, Young Key Shim,† and Sang Joon Choe*

Department of Chemistry, Institute of Basic Science, Inje University, Kimhae 621-749, Korea
**E-mail: chemcsj@inje.ac.kr*
†School of Nano Engineering, Inje University, Kimhae 621-749, USA
Received August 29, 2008, Accepted November 20, 2008

This study reports on the geometry optimizations and electronic structure calculations for methyl pyropheophorbide (MPPa), tropolonyl methyl pyropheophorbides (TMPPa, ITMPPa), and cationic tropolonyl methyl pyropheophorbides ($TMPPa^{-}{\cdot}BF_4^{+}$, $ITMPPa^{+}{\cdot}BF_4^{-}$, $TMPPa^{-}$, and $ITMPPa^{-}$) using Local Spin Density Approximation (LSDA/6-31G*) and the Restricted Hatree-Fock (RHF/6-31G*) level theory. From the calculated results, we found that substituted cationic tropolonyl groups have larger structural effects than those of substituted neutral tropolonyl groups. The order of structural change effects is $ITMPPa^{-}$ > $ITMPPa^{-}{\cdot}BF_4^{+}$ > ITMPPa, as a result of the isopropyl group. Because it is an electron-releasing group, the substituted isopropyl group electronic effect on a 3-position tropolone increases the Highest Occupied Molecular Orbital and Lowest Unoccupied Molecular Orbital (HOMO-LUMO) energy gap. It was constituted that the larger the cationic characters of these photosensitizers, the smaller the HOMO-LUMO band gaps are. The orbital energies of the cationic systems and the ions are stronger than those of a neutral system because of a strong electrostatic interaction. However, this stabilization of orbital energies are counteracted by the distortion of chlorin macrocycle, which results in a large destabilization of chlorin-based compound HOMOs and smaller destabilization of LUMOs as shown in TMPPa (ITMPPa), $TMPPa^{+}{\cdot}BF_4^{-}$ ($ITMPPa^{-}{\cdot}BF_4^{+}$), and $TMPPa^{+}$ ($ITMPPa^{+}$) of Figure 6 and Table 6-7. These results are in reasonable agreement with normal-coordinate structural decomposition (NSD) results. The HOMO-LUMO gap is an important factor to consider in the development of photodynamic therapy (PDT).

Key Words: Tropolonyl methyl pyropheophorbides, Cationic tropolonyl methyl pyropheophorbides, Photodynamic therapy (PDT), DFT

Introduction

Based on porphyrin structures, chlorin-based compound is a more attractive photosensitizer because of its strong absorbance band at 665nm.[1] The subsequent irradiation with visible light and in the presence of oxygen, specifically produces damaged cells that inactivate the microorganisms.[2-5] Generally, gram-positive bacteria are efficiently photoinactivated by a variety of photosensitizers, whereas gram-negative bacteria are resistant to the action of negatively charged or neutral agent.[2] Tropolones have been shown to be bacteriostatic and bactericidal for gram-positive and gram-negative bacterial species.[4] Without the presence of an additional permeability agent, cationic photosensitizer have been shown to photoinduce direct inactivation of gram-negative bacteria.[2,5] Cationic photosensitizer for porphyrin had been investigated by several researchers.[1,6-10]

In a recent study, the combined chlorin-based compounds of novel photosensitizer as PDT and the tropolones as antimicrobials were synthesized to see the dual function activities.[11,12] The combined compounds are tropolonyl methyl pyropheophorbides (TMPPa and ITMPPa) and methyl pyropheophorbide-substituted tropylium tetrafluroborates ($TMPPa^{-}{\cdot}BF_4^{+}$, $ITMPPa^{+}{\cdot}BF_4^{-}$), whose structures have not yet been measured experimentally.

Density functional theory (DFT) have been extensively used to study various aspects of the porphyrin macrocycle,[13(a)] the theoretical studies on photosensitizer are relatively scare. Beck's three parameter hybrid functional using the LYP correlation function (B3LYP) among the DFT is the most popular density functional theory.[21] In previous study,[15] the order of the maximum difference error is HF (Hartree-Fock) > LSDA > B3LYP with respect to experimental for each model chemistry, namely, the B3LYP among the three theory is adequate. It is well-known that the HF method overestimates HOMO-LUMO band gaps as compared to that of other method.[14(b)] To calculate higher accuracy energy models, we need to select a large basis set. It is difficult to calculate with a large basis set for these molecules. However we found that the wavelength owing to B3LYP/6-31G* energy band gaps is favored with experimental value in Soret (B) and local spin density approximation (LSDA/6-31G*) energy band gaps are favored with experimental value in visible bands(Q) in previous study.[15] We are interested in photosensitizers to have a long wavelength from the base on calculated geometries. Thus in this study we carried out LSDA calculations because good photosensitizers may be related to the red shift of the longest wavelength Q band, which enables low energy light to be used.[7] This work is intended to serve as the basis for understanding the distortion of chlorin macrocycle by the tropolonyl group in structural effects and providing the insight of the ground state absorption (Visible band, Q band) from the calculated electronic state.

This paper presents the results of molecular geometries and electronic structures of methyl pyropheophorbide-a (MPPa),

tropolonyl methyl pyropheophorbide-a (TMPPa), 3-isopropyl-tropolone methyl pyropheophorbide-a (ITMPPa), methyl pyropheophorbide-a substituted tropylium terafluoroborate ($TMPPa^+ \cdot BF_4^-$), methyl pyropheophorbide-a substituted 3-isopropyl-tropylium tetrafluoroborate ($ITMPPa^+ \cdot BF_4^-$), methyl pyropheophorbide-a substituted tropylium ion ($TMPPa^-$), and methyl pyropheophorbide-a substituted 3-isopropyltropylium ion ($ITMPPa^-$) using the LSDA/6-31G*//RHF/ 6-31G* level theory.[16] Methyl pyropheophorbide-a-substituted tropylium ions ($TMPPa^-$ and $ITMPPa^+$) were studied to evaluate the structural consequences of electronic oxidation. On the bases of these geometries, we examine their electronic structures, particularly the Kohn-Sham eigenvalues, and the eigenstates of the four orbitals [Next Highest Occupied Molecular Orbital (NHOMO), Highest Occupied Molecular Orbital (HOMO), Lowest Unoccupied Molecular Orbital (LUMO), and Next Lowest Unoccupied Molecular Orbital (NLUMO)] in Gouterman's model.[17]

Furthermore, non-planar deformations of the chlorin macrocycle are induced by steric forces arising from the substituted tropolone and cationic tropolone in methyl pyropheophorbides. The optimized structures were later analyzed using normal-coordinate structural decomposition (NSD).[13(b),18-19] As we examine the effects, the tropolonyl substituents and the deformations of chlorins ring in π system have been related to the visible band.

Computational Methods

DFT calculations were carried out using LSDA.[16] The closed-shell species (MPa, MPPa, TMPPa, ITMPPa, $TMPPa^- \cdot BF_4^-$, $ITMPPa^+ \cdot BF_4^-$, $TMPPa^+$, and $ITMPPa^-$) were calculated with the spin-restricted method. A preliminary search for stationary structures of all studied species was carried out by geometry optimizations using the restricted Hatree-Fock (RHF) level theory. The obtained structures were for the final optimization using the LSDA level theory, then the split-valence and polarized 6-31G* basis set were employed in the geometry optimizations. The Hartree-Fock orbital energies can be used to reproduce ultraviolet photoelectron spectra patterns *via* Koopman's theorem (KT). LSDA is based on densities rather than wave functions, and the Kohn-Sham (KS) orbital energies. Wavelengths of Q band were calculated from Gouterman (the Four Orbitals).[17] Geometries in ions ($TMPPa^-$ and $ITMPPa^-$) were also fully optimized with the SCF=QC option to achieve convergence.

The LSDA-optimized structures are analyzed using NSD.[13(b),18-19] This method characterizes the chlorin conformation in terms of equivalent displacements along the normal coordinates chlorin macrocycle. Typically, the largest static distortions of the chlorin macrocycle occur along the softest normal modes, hence the greatest contributors to the nonplanar distortion are the lowest-frequency normal coordinates of each out-of-plane symmetry type (B_{1u}, B_{2u}, A_{2u}, E_g, and A_{1u}). These deformations correspond to the symmetric distortions commonly observed in a structure and were named ruffling (ruf), saddling (sad), doming (dom), waving (wav(x,y)), and propelling (pro).[13(b),18-19] They give asymme- tric macrocyclic distortions of various types, adding along the projections of the total distortions when mixed together. Only these six normal coordinates typically simulate the actual out-of-plane distortion that is reasonably accurate. The Gaussian 03 program and NSD program on Silicon Graphics Computer System were used in performing calculations and in searching for the optimum geometries using the criteria of minimum energies.[16]

Results and Discussion

Molecular Geometries. The geometries are important because of closely relation with HOMO-LUMO band gaps and the distortion of chlorin macrocycles. Therefore we will be described to bond angles and bond lengths due to (cationic) tropolonyl groups. The structural formulas of methyl pyropheophorbide-a (MPPa) and methyl pheophorbide-a (MPa) are shown in Figure 1. MPPa is obtained when the carboxyl group is decarboxylated in ring V in MPa. The X-ray crystal and molecular structure of MPa was studied by Fischer *et al.* (1972).[20] Figure 2 shows the structural formula of tropolonyl methyl pyropheophorbide-a (TMPPa), 3-isopropyl-tropolone methyl pyropheophorbide-a (ITMPPa). Figure 3 shows the structural formula of cationic photosensitizers. Methyl pyropheophorbide-a-substituted tropylium tetrafluoroborate ($TMPPa^- \cdot BF_4^-$) and

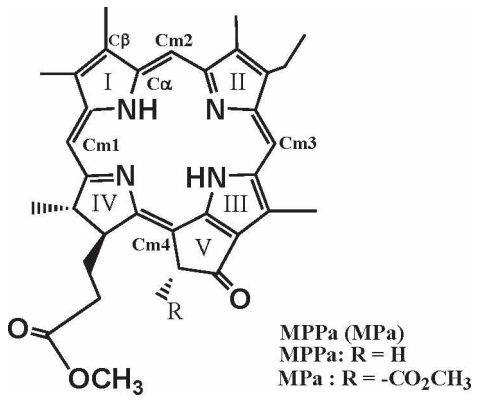

Figure 1. Structural formula of methyl pyropheophorbide-a (MPPa) and methyl pheophorbide-a (MPa)

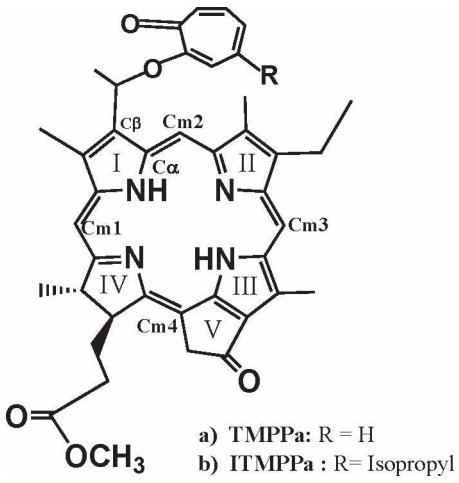

Figure 2. Structural formula of tropolonyl methyl pyropheophorbide-a (TMPPa) and 3-isopropyl-tropolone-methyl pyropheophorbide-a (ITMPPa)

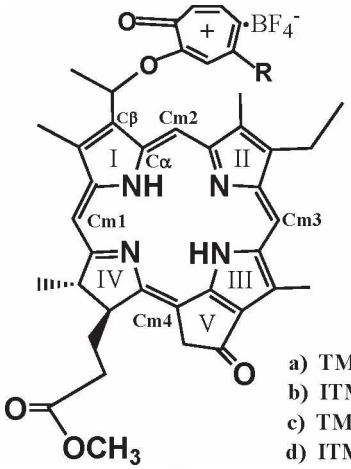

Figure 3. Structural formula of cationic photosensitizers: (a) methyl pyropheophorbide-a-substituted tropylium tetrafluoroborate ($TMPPa^{-}\cdot BF_4^{-}$) (b) methyl pyropheophorbide-a-substituted 3-isopropyl-tropylium terafluoroborate ($ITMPPa^{-}\cdot BF_4^{-}$) (c) methyl pyropheophorbide–a-substituted tropylium ion ($TMPPa^{+}$) (d) methyl pyropheophorbide-a-substituted 3-isopropyl tropylium ion ($ITMPPa^{+}$).

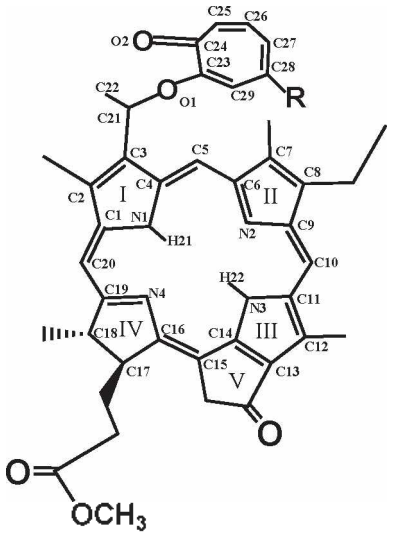

Figure 4. Selected the geometries of tropolonyl methyl pyropheophorbides-a with numerical label.

methyl pyropheo-phorbide-a-substituted 3-isopropyl-tropylium tetrafluoroborate ($ITMPPa^{-}\cdot BF_4^{-}$) were synthesized by Barkhuu.[12] Methyl pyropheophorbide-a-substituted tropylium ion ($TMPPa^{-}$) and methyl pyropheophorbide-a-substituted 3-isopropyl tropylium ion ($ITMPPa^{-}$) are studied to evaluate the structural consequences of electronic oxidation. TMPPa and ITMPPa were obtained when tropolone (or 3-isopropyl tropolone) was combined with MPPa. Selected LSDA-optimized bond distances in methyl (pyro) pheophorbides, tropolonyl methyl pyropheophorbides, and methyl pyropheophorbide-a-substituted tropylium ions are listed in Table 1 in accordance to the numbering shown in Figure 4. The calculated MPa bond lengths are good agreement with the experimental crystal structure of MPa,[20] with a maximum difference of ~0.035 Å. Calculated bond lengths are slightly shorter than the measured ones except C2-C3 in ring I, 0.020-0.022 Å for C1-C2 and C3-C4 bonds, 0.035 Å for C2-C3 bond, and 0.001-0.007 Å for C1-N1

Table 1. Selected Bond Distances(Å) of Chlorin Macrocycle in MPa, MPPa, TMPPa, ITMPPa, $TMPPa^{+}$, and $ITMPPa^{+}$ by LSDA/6-31G*// HF/6-31G* Calculations

	MPa	Exp[a]	MPPa	TMPPa	ITMPPa	$TMPPa^{+}$	$ITMPPa^{+}$
C1-C2	1.426	1.448	1.426	1.437	1.437	1.445	1.435
C2-C3	1.388	1.353	1.388	1.380	1.379	1.375	1.379
C3-C4	1.439	1.459	1.439	1.431	1.432	1.439	1.432
C4-C5	1.381	1.371	1.381	1.383	1.382	1.387	1.389
C5-C6	1.394	1.412	1.394	1.395	1.395	1.390	1.390
C6-C7	1.451	1.429	1.451	1.451	1.451	1.457	1.455
C7-C8	1.366	1.361	1.366	1.366	1.366	1.362	1.364
C8-C9	1.449	1.453	1.446	1.448	1.448	1.457	1.455
C9-C10	1.391	1.376	1.392	1.392	1.392	1.398	1.398
C10-C11	1.387	1.404	1.387	1.388	1.388	1.381	1.382
C11-C12	1.424	1.392	1.427	1.426	1.426	1.442	1.439
C12-C13	1.386	1.398	1.385	1.386	1.386	1.377	1.378
C13-C14	1.414	1.404	1.415	1.415	1.414	1.420	1.418
C14-C15	1.403	1.388	1.402	1.403	1.403	1.399	1.400
C15-C16	1.387	1.390	1.383	1.382	1.382	1.387	1.386
C16-C17	1.516	1.492	1.513	1.513	1.513	1.505	1.507
C17-C18	1.528	1.551	1.533	1.534	1.533	1.534	1.534
C18-C19	1.506	1.490	1.508	1.507	1.507	1.499	1.501
C19-C20	1.385	1.408	1.386	1.387	1.388	1.399	1.395
C1-C20	1.390	1.381	1.390	1.387	1.387	1.378	1.382
C1-N1	1.363	1.364	1.363	1.361	1.360	1.364	1.366
C4-N1	1.365	1.372	1.365	1.367	1.367	1.360	1.363
C6-N2	1.354	1.348	1.354	1.353	1.353	1.359	1.359
C9-N2	1.366	1.373	1.365	1.366	1.366	1.360	1.360
C11-N3	1.383	1.394	1.382	1.382	1.382	1.379	1.379
C14-N3	1.339	1.328	1.340	1.340	1.340	1.341	1.340
C16-N4	1.355	1.347	1.354	1.355	1.355	1.360	1.359
C19-N4	1.344	1.340	1.342	1.341	1.341	1.337	1.339
N1-H21	1.029	-	1.029	1.029	1.029	1.029	1.029
N3-H22	1.041	-	1.043	1.043	1.043	1.041	1.041

[a]Ref 20

and C4-N1 bonds. In ring II, the difference of calculated C8-C9 and C6-C7 bonds from the measured one is 0.004 to 0.022 Å, 0.005 Å for C7-C8 bond, and 0.006-0.007Å for C6-N2 and C9-N2 bonds. The difference of C13-C14 bond from the measured one is 0.010 Å and 0.0321 Å for C11-C12 bond in ring III. In ring IV, the difference of C16-C17 and C18-C19 bonds from measured one is 0.024 Å and 0.016 Å respectively. The difference of C12-C13 bond in ring III and C17-C18 in ring IV is 0.012 Å and 0.023 Å, respectively. In ring III, the difference of C11-N3 and C14-N3 bonds is 0.011 Å and 0.016 Å, respectively. In ring IV, the difference of C16-N4 and C19-N4 bonds is 0.004 Å and 0.008 Å, respectively. The differences of C4-C5, C5-C6, C9-C10, C10-C11, C19-C20, and C1-C20 are 0.01, 0.018, 0.015, 0.017, 0.015, 0.003, 0.023, 0.009 Å, respectively.

To examine validity of bond lengths, we compared the LSDA optimized bond lengths and the HF. The LSDA optimized Mpa bond lengths are the maximum difference of ~ 0.035 Å, whereas the HF optimized MPa bond lengths (see Table 9) are the maximum difference of ~0.058 Å. The LSDA optimized maximum error percentage is 2.6% and 4.3% for HF, respectively. The average of bond length difference of the LSDA optimized Mpa is 0.014 Å and 0.026 Å for the HF optimized and therefore the LSDA optimized MPa bond lengths are more adequate than that of HF.

Compared to that of MPPa, the C1-C2 bond lengths of

TMPPa, ITMPPa, $TMPPa^+$, and $ITMPPa^+$ are extended by 0.011, 0.011, 0.019, and 0.009 Å respectively, owing to the effect on the nearest ring I by the tropolonyl and tropylium group. The C2-C3 and C3-C4 bond lengths have a maximum difference of 0.007 to 0.013 Å, likewise owing to the tropolonyl group and tropylium group effect on the nearest ring I. The bond lengths of TMPPa and ITMPPa have a maximum difference of 0.001 to 0.002 Å in ring II-IV as compared to that of MPPa, owing to the tropolonyl group. The bond lengths of $TMPPa^+$ and $ITMPPa^+$ have a maximum difference of 0.001 to 0.015 Å in ring II-IV as compared to that of MPPa in accordance with the tropylium group. We found that bond lengths caused by the tropylium group effect were larger than those of the tropolonyl group.

The bonds of C4-C5, C5-C6, C9-C10, C10-C11, C19-C20, and C1-C20 in TMPPa and ITMPPa are have a maximum differences of only 0.001 to 0.003 Å, as compared to that of MPPa; whereas for $TMPPa^-$ and $ITMPPa^-$, the maximum is 0.003-0.013.

Table 2 shows selected bond angles in methyl (pyro)pheophorbides, tropolonyl methyl pyropheophorbides, and methyl pyropheophorbide-a-substituted tropylium ions using the LSDA/6-31G*//HF/6-31G* level theory. The calculated bond angles of MPa are in good agreement with the experimental crystal structure of one,[20] with a maximum difference of ~2.2 degrees. In ring I. The C1-C2-C3 and C2-C3-C4 bond angles are increased by 0.4 and 1.6 degrees respectively, as compared to those of the measured one. In ring II-IV, the bond angles of C6-C7-C8, C7-C8-C9, C11-C12-C13, C12-C13-C14, C16-C17-C18, and C17-C18-C19 decrease except for the C12-

Table 2. Selected Bond Angles(°) of Chlorin Macrocycle in Mpa, MPPa, TMPPa, ITMPPa, $TMPPa^-$, and $ITMPPa^+$ by LSDA/6-31 G*//HF/6-31G* Calculations

	MPa	Exp[a]	MPPa	TMPPa	ITMPPa	$TMPPa^-$	$ITMPPa^+$
C1-C2-C3	107.3	106.9	107.3	106.1	106.1	106.2	106.5
C2-C3-C4	107.3	108.9	107.4	108.7	108.6	108.4	108.5
C2-C1-C20	127.0	126.6	127.1	126.7	126.6	125.8	126.5
C3-C4-C5	126.8	126.7	126.5	126.5	126.5	126.5	126.6
C4-C5-C6	128.3	128.8	128.6	128.6	128.6	127.9	128.1
C5-C6-C7	122.3	123.7	122.4	122.5	122.5	122.4	122.6
C6-C7-C8	105.9	106.8	105.9	105.9	105.9	105.8	105.8
C7-C8-C9	105.8	106.6	105.8	105.8	105.8	105.6	105.7
C8-C9-C10	123.8	125.7	124.0	124.1	124.1	123.5	123.6
C9-C10-C11	124.2	125.2	123.9	123.9	123.9	123.6	123.7
C10-C11-C12	129.9	131.1	130.3	130.3	130.4	129.8	129.9
C11-C12-C13	104.9	107.0	105.0	105.0	105.0	104.8	104.8
C12-C13-C14	109.2	107.0	109.0	109.0	109.0	109.2	109.1
C13-C14-C15	113.6	114.5	113.2	113.2	113.2	112.9	113.0
C14-C15-C16	124.0	127.2	124.8	124.9	124.0	124.1	124.4
C15-C16-C17	127.7	126.7	126.6	126.7	126.7	126.5	126.6
C16-C17-C18	100.8	101.6	101.3	101.3	101.3	101.6	101.4
C17-C18-C19	100.7	101.4	101.2	101.2	101.2	101.5	101.3
C18-C19-C20	121.8	123.1	121.9	122.0	122.0	121.5	121.7
C19-C20-C1	127.4	128.8	127.2	127.0	126.9	127.1	127.1
C1-N1-C4	110.5	110.5	110.5	110.2	110.2	110.0	110.4
C6-N2-C9	104.9	106.3	105.0	105.1	105.1	104.6	104.7
C11-N3-C14	109.1	108.9	109.0	109.0	109.0	108.8	108.8
C16-N4-C19	108.2	108.2	108.5	108.5	108.5	107.9	108.0
C1-N1-H21	123.6	-	123.1	123.1	123.1	124.0	123.4
C4-N1-H21	125.9	-	126.4	126.7	126.8	126.1	126.3
C11-N3-H22	118.6	-	118.2	118.1	118.1	118.6	118.6
C14-N3-H22	132.4	-	132.8	132.9	132.8	132.6	132.5
N1-C1-C2	107.8	107.8	107.8	108.2	108.3	108.2	107.8
N1-C4-C3	107.1	105.9	107.0	106.7	106.8	107.3	106.8
N2-C6-C7	111.8	111.4	111.7	111.7	111.7	111.9	111.9
N2-C9-C8	111.7	109.3	111.6	111.5	111.5	112.0	111.9
N3-C11-C12	108.8	107.8	108.8	108.8	108.8	108.9	108.9
N3-C14-C13	107.9	109.3	108.2	108.2	106.1	108.4	108.4
N4-C16-C17	111.1	112.7	111.7	111.7	111.6	112.2	112.1
N4-C19-C18	112.1	113.6	112.4	112.5	112.4	113.3	113.1
N1-C1-C20	125.2	125.2	125.2	125.1	125.2	126.0	125.7
N1-C4-C5	126.1	127.4	126.5	126.8	126.7	126.2	126.6
N2-C6-C5	125.9	124.8	125.9	125.8	125.8	125.7	125.5
N2-C9-C10	124.5	125.0	124.4	124.4	124.4	124.5	124.5
N3-C11-C10	121.2	121.1	120.8	120.8	125.8	121.4	121.3
N3-C14-C15	138.4	136.2	138.6	138.6	140.7	138.7	138.6
N4-C16-C15	121.2	120.5	121.5	121.5	121.5	121.1	121.2
N4-C19-C20	125.9	123.3	125.5	125.4	125.4	125.1	125.1

[a]Ref 20

C13-C14 bond angle, as compared to those of experimental value. The optimized bond angle of C2-C1-C20, C3-C4-C5, C5-C6-C7, C8-C9-C10, C10-C11-C12, C13-C14-C15, C15-C16-C17, and C18-C19-C20 is reduced by 0.1 to 1.4 degrees except for C2-C1-C20, C3-C4-C5 and C15-C16-C17 bond angles. The optimized LSDA bond angle of C4-C5-C6, C9-C10-C11, C19-C20-C1, and C14-C15-C16 is reduced by 0.5 to 3.2 degrees. To examine validity of bond angles, we compared the LSDA optimized Mpa bond angles and the HF. The LSDA optimized Mpa bond angles are the maximum difference of ~ 3.2 degree, whereas the HF optimized MPa bond angles (see Table 10) are the maximum difference of ~4.4 degree. The LSDA optimized maximum error percentage is 2.5% and 3.5% for HF, respectively. The average of bond angles difference of the LSDA optimized Mpa is 1.08 degree and 1.20 degree for the HF optimized and therefore the LSDA optimized MPa bond angles are more adequate than that of HF.

The LSDA-optimized bond angles of MPPa have a maximum difference of ~0.2 degrees, as compared to those of MPa in ring I-III. In ring IV, bond angles (C16-C17-C18, C17-C18-C19) are increased by 0.5 degrees as compared to those of MPa owing to the carboxylated group. The bond angles of C14-C15-C16 and C15-C16-C17 are increased by 0.8 and 1.1 degrees from that of MPa. For the residue angles of MPPa which has a maximum difference of ~0.4 degrees. The bond angles of TMPPa and ITMPPa have a maximum difference of 1.2 ~ 1.3 degrees from MPPa in ring I, however, the bond angles in ring II-IV were not changed. The maximum difference for the residue angles of TMPPa and ITMPPa is ~0.5 degrees. The calculated bond angles of $TMPPa^-$ and $ITMPPa^-$ have a larger difference than those of TMPPa and ITMPPa. The calculated bond angles of $TMPPa^-$ and $ITMPPa^+$ are with difference of 0.8 to 1.1 degrees from MPPa in ring I, while the bond angles in ring II-IV have a maximum difference of ~0.3 degrees. The bond angle differences of C2-C1-C20 of $TMPPa^-$ and ITMPPa are 1.3 and 0.6 degrees from MPPa, respectively because of a substitute isopropyl group effect. The bond angle differences of C4-C5-C6 and C13-C14-C15 are 0.7 degrees for $TMPPa^-$ and 0.5 and 0.4 degrees for ITMPPa, respectively.

The bond angle difference of C10-C11-C12 is 0.5 degrees for TMPPa and 0.4 degrees for ITMPPa. The C16-N4-C19 angle has a diference of 0.6 degrees for $TMPPa^+$ and 0.5 degrees for $ITMPPa^+$. Residue angles have a maximum difference of 0.5 degrees for $TMPPa^-$ and 0.4 degrees for $ITMPP^+$. Table 3 shows the selected bond distances and angles in methyl pyropheophorbide-substituted tropylium tetrafluoroborates ($TMPPa^+{\cdot}BF_4^-$ and $ITMPPa^-{\cdot}BF_4^-$). For $TMPPa^-{\cdot}BF_4^-$, the bond lengths of C1-C2, C2-C3, and C3-C4 have a difference of 0.008~0.01 Å from MPPa in ring I. The bond length of C4-C5 has a difference of 0.003 Å in *meso*-2 position (m2) and 0.07 Å for *meso*-1 position (m1). In ring IV, the bond length of C17-C18 has a difference of 0.002 Å from MPPa. The residue distances are equal to those of MPPa. Comparing the bond lengths of $TMPPa^+{\cdot}BF_4^-$ and TMPPa, they have a difference of 0.001 Å, except C1-C2 and C3-C4. The bond lengths of C1-C2 and C3-C4 have a difference of 0.003 Å and 0.002 Å, respectively. For $ITMPPa^+{\cdot}BF_4^-$, the bond lengths of C1-C2, C2-C3 and C3-C4 have a difference of 0.008-0.009 Å from MPPa in ring I. Furthermore, the residue distances have a maximum difference of 0~0.003 Å. Comparing the bond lengths of $ITMPPa^-{\cdot}BF_4^-$ and ITMPPa, the maximum differ-

Table 3. Selected Bond Distances (Å) and Angles (°) of Chlorin Macrocycle in $TMPPa^-{\cdot}BF_4^-$ and $ITMPPa^+{\cdot}BF_4^-$ by LSDA/6-31G* // HF/6-31G* Calculations

	$TMPPa^-{\cdot}BF_4^-$	$ITMPPa^+{\cdot}BF_4^-$
C1-C2	1.434	1.435
C2-C3	1.380	1.380
C3-C4	1.429	1.430
C4-C5	1.384	1.383
C5-C6	1.394	1.394
C6-C7	1.451	1.451
C7-C8	1.366	1.366
C8-C9	1.448	1.449
C9-C10	1.392	1.393
C10-C11	1.387	1.388
C11-C12	1.427	1.427
C12-C13	1.385	1.385
C13-C14	1.415	1.415
C14-C15	1.402	1.402
C15-C16	1.383	1.383
C16-C17	1.513	1.513
C17-C18	1.535	1.534
C18-C19	1.507	1.506
C19-C20	1.387	1.387
C1-C20	1.397	1.388
C1-N1	1.362	1.361
C4-N1	1.367	1.367
C6-N2	1.353	1.353
C9-N2	1.365	1.365
C11-N3	1.382	1.382
C14-N3	1.340	1.340
C16-N4	1.354	1.355
C19-N4	1.341	1.341
N1-H21	1.029	1.029
N3-H22	1.043	1.043
C1-C2-C3	106.2	106.2
C2-C3-C4	108.8	108.7
C2-C1-C20	126.8	126.7
C3-C4-C5	126.6	126.6
C4-C5-C6	128.7	128.7
C5-C6-C7	122.5	122.5
C6-C7-C8	105.9	105.9
C7-C8-C9	105.8	105.8
C8-C9-C10	124.1	124.1
C9-C10-C11	123.8	123.8
C10-C11-C12	130.3	130.3
C11-C12-C13	105.0	105.0
C12-C13-C14	109.0	109.0
C13-C14-C15	113.2	113.2
C14-C15-C16	124.9	124.9
C15-C16-C17	126.5	126.6
C16-C17-C18	101.4	101.3
C17-C18-C19	101.3	101.2
C18-C19-C20	122.0	122.0
C19-C20-C1	127.1	127.0
C1-N1-C4	110.4	110.3
C6-N2-C9	105.1	105.1
C11-N3-C14	109.0	109.0
C16-N4-C19	108.5	108.5
C1-N1-H21	123.1	123.0
C4-N1-H21	126.6	126.7
C11-N3-H22	118.1	118.2
C14-N3-H22	132.9	132.5

ence is 0~0.002 Å. The bond angle difference of C1-C2-C3 is 1.1 degrees for $TMPPa^{-}\cdot BF_4^{-}$ and $ITMPPa^{+}\cdot BF_4^{-}$. C2-C3-C4 bond angle is 1.4 degrees for $TMPPa^{-}\cdot BF_4^{-}$ and 1.3 for $ITMPPa^{-}\cdot BF_4^{-}$ from MPPa in ring I. The C2-C1-C20 bond angle difference is 0.3 degrees for $TMPPa^{+}\cdot BF_4^{-}$ and 0.4 for $ITMPPa^{+}\cdot BF_4^{-}$. Comparing tropolonyl methyl pyropheophorbides (TMPPa and ITMPPa) with methyl pyropheophorbide a substitute to tropylium tetrafluoroborates ($TMPPa^{+}\cdot BF_4^{-}$ and $ITMPPa^{+}\cdot BF_4^{-}$) for residue angles, the maximum angle difference is 0~0.2 degrees except for the angle C14-C15-C16 and C14-N3-H22. The angle differences of C14-C15-C16 and C14-N3-H22 are 0.9 degrees and 0.3 degrees, respectively.

Table 4 shows the distances (Å) between protonated nitrogens and unprotonated nitrogen in a chlorin ring of calculated molecular systems. The distances of protonated nitrogen caused by substituted tropolonyl and cationic tropolonyl are decreased from those of MPa, whereas the unprotonated nitrogen is increased. Particularly, the distances of protonated nitrogen caused by substituted cationic tropolonyl groups are 4.024 Å for $TMPPa^{-}$ and 4.032 Å for $ITMPPa^{-}$ all other molecules are 4.044-4.046 Å. The unprotonated nitrogen distances are 4.151 Å for $TMPPa^{-}$ and 4.159 Å for $ITMPPa^{-}$ all other molecules are 4.170-4.173 Å except for MPa.

Table 4. The distances(Å) between Protonated Nitrogens and between Unprotonated Nitrogens in Chlorin rings of Calculated Molecular Systems

LSDA/6-31G*//HF/6-31G*		
Molecules	NH-NH[a]	N-N[b]
MPa	4.055	4.148
MPPa	4.045	4.171
TMPPa	4.045	4.171
ITMPPa	4.044	4.170
TMPPa+	4.024	4.151
ITMPPa+	4.032	4.159
$TMPPa^{-}\cdot BF_4^{-}$	4.045	4.173
$ITMPPa\cdot BF_4^{-}$	4.046	4.170

[a]NH-NH: The distances between protonated nitrogen in (pyro)pheophorbides rings of molecules, [b]N-N: The distances between unprotonated nitrogen in (pyro)pheophorbides rings

Table 5 shows the selected structural parameters of the tropolonyl groups and the cationic tropolonyl groups in TMPPa, ITMPPa, $TMPPa^{-}$, $ITMPPa^{+}$, $TMPPa^{+}\cdot BF_4^{-}$, and $ITMPPa^{+}\cdot BF_4^{-}$ by LSDA/6-31G*//HF/6-31G* calculations. In order to understand substituted cationic tropolonyl group effects, we compared the substituted tropolonyl groups (TMPPa, ITMPPa) and the cationic tropolonyl groups ($TMPPa^{-}$, $ITMPPa^{-}$, $TMPPa^{-}\cdot BF_4^{-}$, $ITMPPa^{-}\cdot BF_4^{-}$). The dihedral angles are more or less similar in molecular systems except $ITMPPa^{-}$. The C26-C27 bond length of $ITMPPa^{-}$ has maximum difference of 0.078 Å from that of ITMPa. Comparing $TMPPa^{+}$ and $ITMPPa^{-}$ for substituted isopropyl group effects, we found that the dihedral angles of C23-O1-C21-C3 and C23-O1-C21-C22 have large difference of 91.4 degree and 91.2 degree respectively. The bond angle of C25-C26-C27 has maximum difference of 32.7 degree. The order of structural effects owing to the isopropyl group is $ITMPPa^{+}$ > $ITMPPa^{-}\cdot BF_4^{-}$ > ITMPPa. We further found that substituted cationic tropolony groups are with larger structural effects than the tropolonyl group. Although the dihedral angles are large change by tropolonyl group, the distortion of chlorin macrocycle is not great influence because

Table 5. Selected (Cationic) Tropolonyl groups Structural Parameters of TMPPa, ITMPPa, $TMPPa^{+}$, $ITMPPa^{-}$, $TMPPa^{-}\cdot BF_4^{-}$, and $ITMPPa^{-}\cdot BF_4^{-}$ by LSDA/6-31G*//HF/6-31G* Calculations

	TMPPa	ITMPPa	$TMPPa^{-}$	$ITMPPa^{+}$	$TMPPa^{+}\cdot BF_4^{-}$	$ITMPPa^{-}\cdot BF_4^{-}$
Dihedral angle(°)						
C23-O1-C21-C3	161.1	163.0	161.2	69.8	161.2	162.4
C29-C23-O1-C21	-1.8	-3.1	-2.7	8.1	-1.93	-3.0
C24-C23-O1-C21	178.6	177.5	177.4	-166.2	178.4	177.4
O2-C24-C23-O1	-0.8	-0.3	-2.0	11.2	-3.2	-0.6
C23-O1-C21-C22	-77.3	-75.3	-76.9	-168.1	-77.2	-75.8
C23-C24-C25-C26	0.1	0.3	1.3	25.7	5.3	0
C24-C25-C26-C27	-0.1	-0.3	-0.9	-20.1	-0.5	-0.8
C25-C26-C27-C28	0.1	-0.3	2.9	-19.2	-5.5	1.3
C26-C27-C28-C29	0.2	0.5	-3.8	26.4	4.4	-0.8
C27-C28-C29-C23	-0.7	0.2	1.6	-30.7	0.3	0.1
Bond distance(Å)						
C23-C24	1.482	1.481	1.498	1.501	1.439	1.486
C24-C25	1.439	1.437	1.441	1.477	1.443	1.441
C25-C26	1.368	1.368	1.377	1.309	1.365	1.346
C26-C27	1.409	1.408	1.363	1.330	1.388	1.385
C27-C28	1.371	1.375	1.330	1.425	1.352	1.375
Bond angle (°)						
C23-C24-C25	121.9	121.3	124.4	116.6	122.8	120.8
C24-C25-C26	132.3	131.8	130.0	116.3	131.7	127.6
C25-C26-C27	129.8	130.5	121.0	153.7	125.1	139.0
C26-C27-C28	127.0	128.3	145.1	115.2	135.6	123.3
C27-C28-C29	129.5	126.5	120.8	121.3	125.3	126.8
C28-C29-C23	130.1	131.8	127.6	131.1	129.3	132.5
C23-O1-C21	122.6	122.4	122.5	122.9	122.8	122.6

troponlonyl group is antimcrobials. The PDT activity only depends on the distortion of chlorine mcrocycle.

Tropolonyl group is added as antimicrobials to see the dual function activities of PDT. The difference of bond lengths and bond angles from the MPPa means that chlorin macrocycle on molecular systems may be influence to the distortion by the substituted structural effects of tropolonyl group, although by a small amount.

Electronic Structures

Table 6 shows the reversed eigenvalues (in eV), Gouterman's four orbitals[17] [NHOMO (b2), HOMO (b1), LUMO (c1), and NLUMO (c2)] calculated by Hartree-Fock (HF), and the LSDA theory for MPa, MPPa, TMPPa, and ITMPPa. The $\Delta\varepsilon_{hl}$ and $\Delta\varepsilon_{hnl}$ are the states associated with visible bands.[17] $\Delta\varepsilon_{hl}$ and $\Delta\varepsilon_{hnl}$ energy gaps for MPa are 1.610 eV and 2.256 eV, respectively. The $\Delta\varepsilon_{hl}$ ($\Delta\varepsilon_{hnl}$) of MPPa, TMPPa, and ITMPPa are 1.635 (2.255) eV, 1.671(1.933) eV, and 1.672(2.061) eV, which correspond to wavelength of 758(550) nm, 742(641) nm, and 741(601) nm respectively. The wavelength caused by the LSDA energy gaps show 3 ~ 12% deviations from the experimental value in Q bands. However, owing to the tropolonyl groups, the wavelengths of TMPPa and ITMPPa are slightly blue shift as compared to that of MPPa. These tendencies are in reasonable agreement with the experimental value.[11,12] Table 7 shows the sign reversed eigenvalues (in eV), Gouterman's four orbitals.[17] [NHOMO(b2), HOMO(b1), LUMO(c1), and NLUMO(c2)] calculated by Hartree-Fock (HF) and LSDA theory for $TMPPa^{+}\cdot BF_4^{-}$, $ITMPPa^{-}\cdot BF_4^{-}$, $TMPPa^{+}$, and $ITMPPa^{-}\cdot BF_4^{-}$. The calculated $\Delta\varepsilon_{hl}$ ($\Delta\varepsilon_{hnl}$) of $TMPPa^{+}\cdot BF_4^{-}$, $ITMPPa^{+}\cdot BF_4^{-}$, $TMPPa^{-}$, and $ITMPPa^{-}$ are 1.228 (1.666) eV, 1.420 (1.667), 0.013 (1.701) eV, and 0.072 (1.695) eV, respectively. The HOMO-LUMO band gaps ($\Delta\varepsilon_{hl}$) of cationic photosensitizers ($TMPPa^{+}\cdot BF_4^{-}$, $ITMPPa^{-}\cdot BF_4^{-}$, $TMPPa^{-}$, and $ITMPPa^{+}$) were reduced as compared to those of TMPPa and ITMPPa, owing to tropylium tetrfluoroborates and tropylium ions. However, HOMO-LUMO band gaps have less compared to the wavelengths having the larger number. The wavelengths corresponding to the band gaps are red shift. Thus, cationic photosensitizers in Table 7 are better than the neutral photosensitizers in Table 6, because the number of band gaps is small. The isopropyl group, being the electron donor, neutralized photosensitizers. Therefore the HOMO- LUMO band gaps ($\Delta\varepsilon_{hl}$) of TMPPa, $TMPPa^{+}\cdot BF_4^{-}$ and $TMPPa^{-}$ are smaller

Table 6. The Sign reversed eigenvalues (in eV) Gouterman's four orbital [NHOMO(b2) to NLUMO(c2)] calculated using LSDA// RHF level theory. The last two row are the HOMO-LUMO Gap ($\Delta\varepsilon_{hl}$) and NHOMO-LUMO ($\Delta\varepsilon_{hnl}$). Calculated $\Delta\varepsilon_{hl}$ and $\Delta\varepsilon_{hnl}$ are the state associated with visible band, parentheses are wavelengths (in nm).

	LSDA/6-31G*//RHF/6-31G*			
	MPa	MPPa	TMPPa	ITMPPa
b2	5.422	5.281	5.289	5.277
b1	5.357	5.228	5.206	5.191
c1	3.747	3.593	3.535	3.519
c2	3.101	2.973	3.273	3.130
Exp[a]	1.856(668)	1.858(667)	1.867(664)	1.870(663)
Cal				
$\Delta\varepsilon_{hl}$	1.610(770)	1.635(758)	1.671(742)	1.672(741)
$\Delta\varepsilon_{hnl}$	2.256(550)	2.255(550)	1.933(641)	2.061(601)

[a]ref 11-12

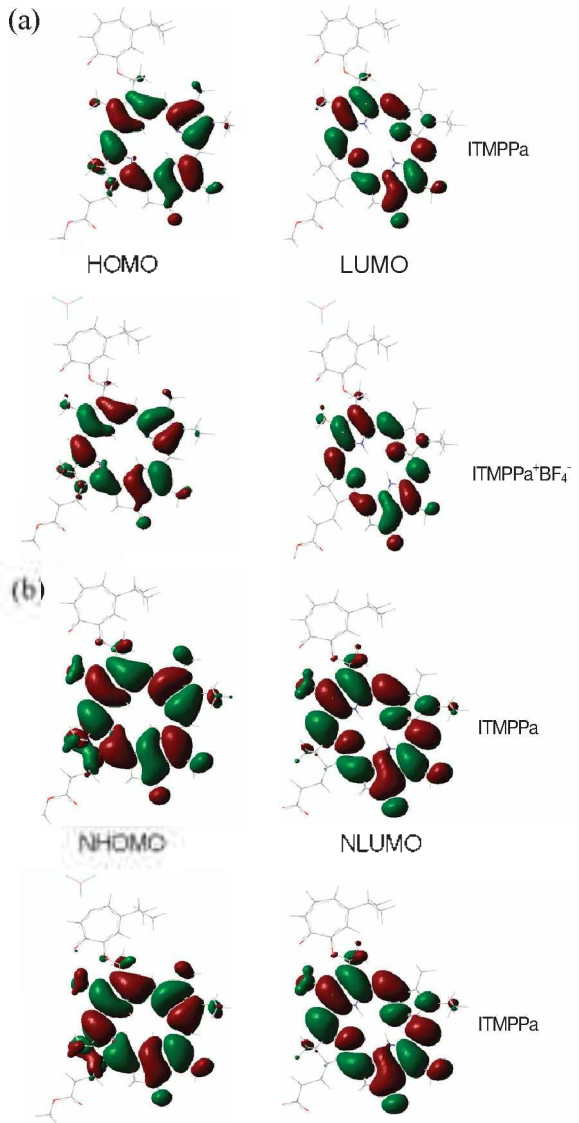

Figure 5. The molecular orbital contours of the HOMO, LUMO, NHOMO, and NLUMO for ITMPPa and $ITMPPa^{-}\cdot BF_4^{-}$, calculated from the LSDA theory. (a) HOMO and LUMO for wave function 0.02 a.u; (b) NHOMO and NLUMO for wave function 0.01 a.u.

Table 7. The Sign reversed eigenvalues (in eV) Gouterman's four orbital [NHOMO(b2) to NLUMO(c2)] calculated using LSDA//RHF. Calculated $\Delta\varepsilon_{hl}$ and $\Delta\varepsilon_{hnl}$ are the state associated with visible band.

	LSDA/6-31G*//RHF/6-31G*			
	$TMPPa^{-}\cdot BF_4^{-}$	$ITMPPa^{-}\cdot BF_4^{-}$	$TMPPa^{-}$	$ITMPPa^{-}$
b2	5.461	5.476	8.048	7.967
b1	5.387	5.397	7.934	7.916
c1	4.159	3.978	7.921	7.844
c2	3.720	3.730	6.233	6.220
Cal				
$\Delta\varepsilon_{hl}$	1.228	1.420	0.013	0.072
$\Delta\varepsilon_{hnl}$	1.666	1.667	1.701	1.695

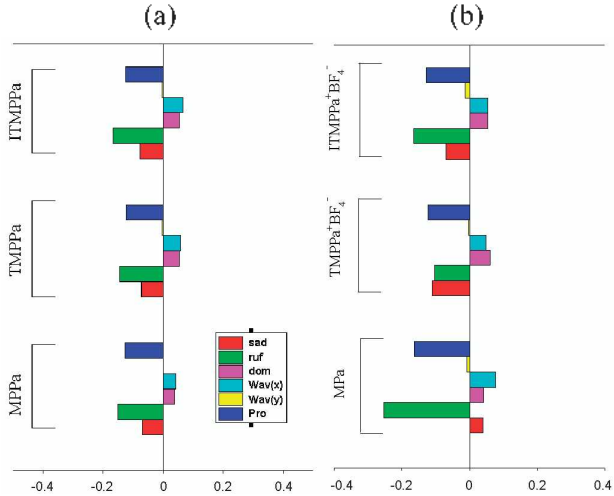

Figure 6. Out-of-plane deformations (in Å) for calculated LSDA of molecular systems: (a) the deformations of MPPa, TMPPa, ITMPPa. (b) The deformations of MPa, TMPPa$^+$·BF_4^-, and ITMPPa$^+$·BF_4^-.

Table 8. Selected atomic coefficients of HOMO and LUMO of ITMPPa and ITMPPa$^+$·BF_4^-, all AOs are for orbital 2Pz.

	HOMO		LUMO	
	ITMPPa	ITMPPa$^+$·BF_4^-	ITMPPa	ITMPPa$^+$·BF_4^-
N1	-0.049	-0.049	0.000	0.011
N2	-0.044	-0.043	0.165	0.000
C3	0.058	0.000	0.135	0.000
C4	0.199	0.018	0.148	-0.001
C5	0.047	0.000	-0.156	-0.004
C6	-0.191	-0.190	-0.093	0.005
C7	-0.099	-0.090	0.012	0.004

than those of ITMPPa, ITMPPa$^+$·BF_4^- and ITMPPa$^+$. Thus the larger the cationic character of these photosentizers, the smaller the HOMO-LUMO band gaps is.

Figure 5 shows the three-dimensional (3-D) contours of the Gouterman four orbitals with a wave-function value of 0.01 and 0.02 a.u. for ITMPPa and ITMPPa$^+$·BF_4^- derived from the LSDA theory. The HOMO is delocalized on chlorin macrocycle and has not contributions from (cationic) tropolonyl groups. The LUMO is similar to the HOMO, but the LUMO orbitals on the C17-C18 carbon atoms in ring IV have not contributions. Table 8 lists the selected atomic coefficients of HOMO and LUMO of ITMPPa and ITMPPa$^+$·BF_4^-. It is shown that all the significant atomic orbitals 2Pz for either C or N, suggesting that HOMOs and LUMOs are π orbitals. The atomic coefficients of HOMOs and LUMOs in cationic photosensitizers are smaller than those of neutral photosensitizer. Nevertheless, the eigenvalues of HOMOs and LUMOs of cationic photosensitizers are larger than the neutral one because cationic systems have strong electrostatic interactions as shown in Table 7. And because of the ionic states, TMPPa$^+$ and ITMPPa$^+$ have a very strong electrostatic interaction.

In order to estimate the non-planar deformations of the chlorin macrocycle caused by the substituded tropolone and cationic tropolone in methyl pyropheophorbides, we were analyzed using NSD.[13(b),18-19] Furthermore, the calculated structures (MPPa, TMPPa, ITMPPa, MPa, TMPPa$^+$·BF_4^-, and ITMPPa$^+$·BF_4^-)[13(b),18-19] were analyzed using NSD as shown in Figure 6. First comparing MPa with MPPa compound, non-planar deformations of MPa were larger than those of MPPa. However, because of the carboxyl group effect in ring V of MPa as shown in Figure 1, the HOMO- LUMO band gap of MPa is a slightly smaller than that of MPPa. On the other hand, NSD results show a larger change in out-of-plane deformation at TMPPa than that of MPPa to some extent. From detailed NSD results of MPPa, saddling is -0.070 A, ruffling is -0.152 A, doming is 0.037 A, wav(x) is 0.043 A, wav(y) is 0.001 A, and pro is -0.127 A. In contrast, saddling of TMPPa is -0.073 A, -0.146 A for ruffling, 0.054 A for doming, 0.058 A for wav(x), -0.004 A wav(y), and -0.124 A for pro. Hence, total observed distortion of MPPa is 0.218 A, compared to that of TMPPa, which is 0.219 A. It means that the HOMO-LUMO band gap is in reasonable agreement with the NSD results in MPPa and TMPPa.

Table 9. Selected Bond Distances(Å) of Chlorin Macrocycle in MPa and MPPa by HF/6-31G* Calculation

	MPa	MPPa		MPa	MPPa
C1-C2	1.477	1.477	C15-C16	1.339	1.336
C2-C3	1.340	1.340	C16-C17	1.529	1.527
C3-C4	1.476	1.476	C17-C18	1.543	1.546
C4-C5	1.342	1.343	C18-C19	1.517	1.519
C5-C6	1.449	1.449	C19-C20	1.441	1.442
C6-C7	1.473	1.472	C1-C20	1.351	1.350
C7-C8	1.343	1.344	C1-N1	1.360	1.361
C8-C9	1.469	1.468	C4-N1	1.373	1.373
C9-10	1.347	1.349	C6-N2	1.293	1.293
C10-C11	1.435	1.434	C9-N2	1.394	1.394
C11-C12	1.381	1.383	C11-N3	1.387	1.385
C12-C13	1.418	1.417	C14-N3	1.325	1.326
C13-C14	1.375	1.375	C16-N4	1.405	1.404
C14-C15	1.451	1.450	C19-N4	1.283	1.281
N1-H21	0.992	0.992	N3-H22	0.993	0.992

Table 10. Selected Bond Angles(°) of Chlorin Macrocycle in MPa and MPPa by HF/6-31G* Calculation

	MPa	MPPa		MPa	MPPa
C1-C2-C3	107.9	107.9	C11-N3-C14	109.1	109.1
C2-C3-C4	108.4	108.4	C16-N4-C19	109.5	109.7
C2-C1-C20	125.6	125.7	C1-N1-H21	124.5	124.4
C3-C4-C5	126.6	126.5	C4-N1-H21	123.7	123.9
C4-C5-C6	126.3	126.5	C11-N3-H22	123.5	123.4
C5-C6-C7	122.9	122.9	C14-N3-H22	127.3	127.5
C6-C7-C8	105.8	105.8	N1-C1-C2	106.3	106.2
C7-C8-C9	106.1	106.1	N1-C4-C3	105.7	105.6
C8-C9-C10	125.9	125.9	N2-C6-C7	112.5	112.4
C9-C10-C11	127.5	127.4	N2-C9-C8	109.3	109.3
C10-C11-C12	129.4	129.8	N3-C11-C12	108.7	108.7
C11-C12-C13	105.1	105.2	N3-C14-C13	108.7	108.9
C12-C13-C14	108.3	108.1	N4-C16-C17	108.4	109.0
C13-C14-C15	114.5	114.4	N4-C19-C18	113.9	114.0
C14-C15-C16	124.8	125.2	N1-C1-C20	128.1	128.1
C15-C16-C17	131.1	130.0	N1-C4-C5	127.8	127.9
C16-C17-C18	100.9	101.1	N2-C6-C5	124.6	124.7
C17-C18-C19	100.3	100.6	N2-C9-C10	124.8	124.8
C18-C19-C20	119.7	120.0	N3-C11-C10	121.9	121.6
C19-C20-C1	127.4	127.2	N3-C14-C15	136.8	136.7
C1-N1-C4	111.7	111.7	N4-C16-C15	120.3	120.9
C6-N2-C9	106.3	106.4	N4-C19-C20	126.4	120.0

Comparing TMPPa and ITMPPa, the distortion of ITMPPa is larger than that of MPPa because of the isopropyl group, which is an electron leaving group. Cationic tropolonyl groups have smaller distortions than tropolonyl groups, comparing cationic tropolonyl methyl pyropheophorbides with tropolonyl methyl pyropheophorbides in Figure 6. The major distortions of TMPPa are -0.073 Å for saddling, -0.146 Å for ruffling, and -0.124 Å for pro. However, those of $TMPPa^{+}\cdot BF_4^{-}$ are -0.109 Å for saddling, -0.103 Å for ruffling, and -0.121 Å for pro. Total observed distortion of $TMPPa^{-}\cdot BF_4^{-}$ is 0.207 Å. The major distortions of ITMPPa are -0.077 Å for saddling, -0.168 Å for ruffling, and -0.126 Å for pro, whereas those of $ITMPPa^{-}\cdot BF_4^{-}$ are -0.069 Å for saddling, -0.165 Å for ruffling, and -0.127 Å for pro.

Table 6-7 shows that the electronic effect of cationic tropolonyl groups reduces the HOMO-LUMO gap. The wavelength corresponding to the band gap increases the red shift.

Conclusion

1. We found the following results from the geometry optimization by LSDA/6-31G*//HF/6-31G* calculation.
   a) After calculating the bond lengths and bond angles, we compared the results of MPa and the experimental MPa. The results are somewhat equivalent with a maximum difference of 0.000-0.035 Å and 0.0-3.2 degrees (see Table 1-2).
   b) TMPPa and ITMPPa which were linked with tropolone change C-C bond lengths of the nearest ring I by 0.007 to 0.011 Å. The C1-C2-C3 bond angles and C2-C3-C4 have a difference of 1.2 degree and 1.3 degree respectively. Other bond lengths have a maximum difference of 0.001-0.003, and the bond angles have a maximum difference 0.5 degrees except the C14-C15-C16 bond angles of ITMPPa (Table 2).
   c) $TMPPa^{+}$ and $ITMPPa^{-}$, which were linked with tropylium ions, changed the C-C bond lengths of the nearest ring I by 0.000 to 0.019 Å. The C1-C2-C3 bond angles and C2-C3-C4 are 0.8 to 1.1 degrees. Other bond lengths have a maximum difference of 0.001-0.011 Å. The bond angles have a maximum difference of ~1.3 degrees (Table 2). $TMPPa^{-}\cdot BF_4$ and $ITMPPa^{+}\cdot BF_4$, which were linked with cationic tropolone, changed the C-C bond lengths of the nearest ring I by 0.008 to 0.010 Å. The C1-C2-C3 bond angles and C2- C3-C4 have a difference of 1.1 to 1.4 degrees. Other bond lengths have a maximum difference of 0.000-0.007 Å. The bond angles have a maximum difference of ~0.4 degrees (Table 3).
2. The electronic effect of cationic tropolonyl groups reduces the HOMO-LUMO band gap. On the other hand, the isopropyl group effect increases the HOMO-LUMO band gaps.
3. The calculated energy band gaps are in reasonable agreement with the experimental value in visible bands (Q) (see Table 6)
4. The distortions of chlorin macrocycle are able to explain the normal-coordinate structural decomposition and the results are in reasonable agreement with the HOMO-LUMO energy gap.
5. The HOMO-LUMO gap is an important factor to consider in the development of PDT.

Acknowledgments. The authors whish to acknowledge financial from Ministry of Education (BK21).

References

1. Webber, J.; Leeson, B.; Fromm, D.; Kessel, D. *J. Photochem. Photobiol.* **2005**, *78*, 135.
2. Caminos, D.; Spesia, B.; Durantini, E. *Photochem. Photobiol. Sci.* **2006**, *5*, 56.
3. DeRosa, M. R.; Crutchley, R. J. *Coord. Chem. Rev.* **2002**, *233-234*, 351.
4. Trust, T. J. *Antimicrob. Agents Chemother.* **1975**, *7*, 500.
5. Nitzan, Y.; Ashkenazi, H. *Curr. Microbiol.* **2001**, *42*, 408.
6. Villanueva, A. *J. Phtochem. Phorobiol.* **1993**, *18*, 295.
7. (a) Ali, H.; van Lier, E. *J. Chem. Rev.* **1999**, *99*, 2379. (b) Jasat, A.; Dolphin, D. *Chem. Rev.* **1997**, *97*, 2267.
8. Garbo, G. M.; Fingar, V. H.; Wieman, T. J.; Noakes III, E. B.; Haydon, P. S.; Cerrito, P. B.; Kessel, D. H.; Morgan, A. R. *Photochem. Photobiol.* **1998**, *68*, 561.
9. Ravanat, J.; Cade, J.; Araki, K.; Toma, H. E.; Medeiros, M. H. G.; Mascio, P. D. *Photochem. Photobiol.* **1998**, *68*, 698.
10. Guiaev, A. B.; Leontis, N. B. *Biochem.* **1999**, *38*, 15425.
11. Bold, B.; Barkhuu, B.; Lee, W.; Shim, Y. K. *Bull. Korean Chem. Soc.* **2008**, *29*, 237.
12. Barkhuu, B. *Develoment and Activity Tests of New Cationic Chlorins for Photodynamic Cancer Therapy*, Thesis for Ph. D; Inje University, Korea, 2007.
13. (a) Ghosh, A. In *The Porphyrin Handbook*; Kardish, K. M.; Smith, K. M.; Guilard, R., Eds.; Academic Press: New York, 2000; Vol. 7, p 1. (b) Shelnutt, J. A. In *The Porphyrin Handbook*; Kardish, K. M.; Smith, K. M.; Guilard, R., Eds.; Academic Press: New York, 2000; Vol. 7, p 167. (c) Pandey, R. K.; Zheng, G. In *The Porphyrin Handbook*; Kardish, K. M.; Smith, K. M.; Guilard, R., Eds.; Academic Press: New York, 2000; Vol. 6, p 158.
14. (a) Takeuchi, T.; Gray, H. B.; Goddard III, W. A. *J. Am. Chem. Soc.* **1994**, *116*, 9730. (b) Wang, Z.; Day, P. N.; Pachter, R. *J. Chem. Phys.* **1998**, *108*, 2504.
15. Park, S. H.; Kim, S. J.; Kim, J. D.; Park, S.; Huh, D. S.; Shim, Y. K.; Choe, S. J. *Bull. Korean Chem. Soc.* **2008**, *29*, 1141.
16. Frisch, M. J.; Trucks, G. W.; Schlegel, H. B.; Gill, P. M. W.; Johnson, B. G.; Robb, M. A.; Cheeseman, J. R.; Keith, T.; Peterson, G. A.; Montgometry, J. A.; Raghavacari, K.; Al-Laham, M. A.; Zakrzewski, V. G.; Ortiz, J. V.; Foresman, J. B.; Cioslowski, J.; Stefanov, B. B.; Nanayakkara, A.; Challacombe, M.; Peng, C. J.; Ayala, P. Y.; Chen, W.; Wong, M. W.; Andres, J. L.; Replogle, E. S.; Gomperts, R.; Martin, R. L.; Fox, D. L.; Binkley, J. S.; Defrees, D. J.; Baker, J.; Stewart, J. P.; Head-Gordon, M.; Gonzalez, C.; Pople, J. A. Gaussian, Inc.: Wallingford, CT, 2005.
17. Gouterman, M. *J. Mol. Spectrosc.* **1961**, *6*, 138.
18. Shelnutt, J. A.; Song, X. Z.; Ma, J. G.; Jia, S. L.; Jentzen, W.; Medforth, C. *J. Chem. Soc. Rev.* **1998**, *27*, 31.
19. Jentzen, W.; Ma, J. G.; Shelnutt, J. A. *Biophys. J.* **1998**, *74*, 753.
20. Fischer, M.; Templeton, D.; Zalkin, A.; Calvin, M. *J. Am. Chem. Soc.* **1972**, *94*, 3613.
21. Zhao, Y.; Truhlar, D. *Acc. Chem. Res.* **2008**, *41*, 157.